Radiation Measurements 82 (2015) 115–121

Contents lists available at ScienceDirect

Radiation Measurements

journal homepage: www.elsevier.com/locate/radmeas

Time and dose-rate dependence of TL and OSL due to competition between excitation and fading

R. Chen [a, *], V. Pagonis [b], J.L. Lawless [c]

[a] Raymond and Beverly Sackler School of Physics and Astronomy, Tel-Aviv University, Tel-Aviv 69978, Israel
[b] Physics Department, McDaniel College, Westminster, MD 21157, USA
[c] Redwood Scientific Incorporated, Pacifica, CA 94044-4300, USA

HIGHLIGHTS

- Competition between excitation and thermal fading of TL and OSL.
- Non-monotonic dependence on the time of excitation.
- Simulations by numerical solution of the relevant coupled differential equations.
- Comparison to quasi-analytical results.

ARTICLE INFO

Article history:
Received 3 June 2015
Received in revised form
19 August 2015
Accepted 23 September 2015
Available online 28 September 2015

Keywords:
Thermoluminescence
OSL
Excitation-fading competition

ABSTRACT

During the excitation period of thermoluminescence (TL) and optically stimulated luminescence (OSL), competing effects of fading may take place, in particular in situations of long irradiation with a relatively low dose rate. In this work, we study, by the use of numerical simulations, this possible occurrence, using a model with two trapping states and one recombination center. The dependence on the time of excitation of the filling of the active trap, to which the TL or OSL signal is proportional, has been followed. Using plausible sets of trapping parameters, the solution of the relevant set of coupled differential equations revealed a time dependence of an increase up to a maximum value and then a decrease toward an equilibrium value where the rates of production and decay are equal. The equilibrium value reached by the simulations has been found to be consistent with a direct comparison of the excitation and the thermal decay rates. The results are somewhat similar to previous reports on non-monotonic dose dependence with two main differences. The previous model included two trapping states and two centers whereas the present one has only one center. Also, previously, the dependence was on the dose with no distinction whether its variation is by changing the dose rate of excitation or the length of irradiation. With the present work, the non-monotonic and final equilibrium behavior have been specific to the time dependence whereas when the dose was varied by changing the dose rate, the curve increased monotonically until it reached the saturation value. Similar results have been reached by a quasi-analytical method, using some plausible simplifying assumptions.

1. Introduction

In the applications of thermoluminescence (TL) and optically stimulated luminescence (OSL) in dosimetry and in dating of archaeological and geological samples, a crucial question is the stability of the measured signal with time. In most cases, some fading is observed which may be normal or anomalous. In normal fading at ambient temperature, trapped carriers are released thermally in accordance with the trapping parameters, thus reducing the expected signal which is associated with the number of trapped carriers at the instance of readout, heating in TL or exposure to stimulating light in OSL. The dependence of the measured signal on the time elapsed between excitation by ionizing radiation and the readout has been discussed in the literature; exponential and non-exponential functions of decay have been reported. It seems obvious that the element of fading takes place during the irradiation as well

* Corresponding author.
E-mail address: chenr@tau.ac.il (R. Chen).

http://dx.doi.org/10.1016/j.radmeas.2015.09.006
1350-4487/

and it may be noticeable in particular in cases where the excitation dose rate is low and the time of excitation is long. In the present work, we study the possibility that accumulation of trapped carriers may not behave in the "normal" linear-sublinear-saturation manner due to fading during the excitation period. It will be shown that under the mentioned circumstances, the TL or OSL signal may behave in such unusual way, namely, it will go up with excitation time up to a certain point, decrease during further excitation time and reach an equilibrium level, lower than the otherwise expected saturation value.

An effect of non-monotonic dose dependence of TL and OSL has been reported by a number of authors and in several materials. Charlesby and Partridge (1963) have described a decline of the maximum TL intensity in γ-irradiated polyethylene at 10^4 Gy and postulated that the cause of the effect is radiation damage. Halperin and Chen (1966) have described the UV excited TL in semiconducting diamonds. The secondary peak at 150 K increased linearly with the dose at low doses, reached a maximum at a certain dose and decreased at high doses. It is quite obvious that in diamonds, photons with energy of 3–5.5 eV cannot cause radiation damage. Cameron et al. (1966) have reported a non-monotonic dose dependence in LiF:Mg,Ti as a function of ^{60}Co γ-ray excitation dose. They have reported on a rather broad range of linear dependence, followed by a superlinear range, after which a maximum value and a decline are observed. Jain et al. (1975) have described a significant decrease of the TL output of peak V in LiF, by a factor of 2.5 from the maximum, and ascribed it to radiation damage. Their graphs have shown that at very high doses, the dose–dependence curves tend to level off following a range of significant decrease in the TL intensity. Similar non-monotonic results have been reported by Horowitz et al. (1986). The effect of non-monotonic dose dependence has also been seen in quartz, the main material used for archaeological and geological dating. Ichikawa (1969) has found that in γ-irradiated natural quartz, the peak at ~200 °C has reached a maximum at 6×10^4 Gy and decreased at higher doses by a factor of ~2.5. Damm and Opyrchal (1975) have reported on TL of γ-irradiated KCl crystals, and described a non-monotonic dose dependence of some of the pure and Sr- and Pb-doped samples. David et al. (1977) and David and Sunta (1981) have shown the dose dependence of some TL peaks in γ-irradiated pink quartz, which revealed a decline following a maximum at 10^3–10^4 Gy. A number of authors have reported on the non-monotonic effect in the important dosimetric material Al_2O_3:C. For example, Yukihara et al. (2003) have described a somewhat superlinear dependence up to ~39 Gy of β-irradiation of the 450 K peak in some of the samples. The peak has reached a maximum value and declined at higher doses. A non-monotonic dependence of TL of γ-irradiated silica glass has been found by Gulamova et al. (1993). This was associated with the behavior of optical absorption at 550 nm. Vij et al. (2009) have reported a non-monotonic dose dependence of TL in SrS:Ce excited by UV light. Similar non-monotonic effects of OSL have been discussed in the literature. For example, Schulman et al. (1957) described the changes in photoluminescence due to prior γ excitation in organic solids. In naphtalene, the dependence of the 464 nm emission stimulated by 365 nm light depended non-linearly on the γ-excitation dose, reaching a maximum at ~10^5 Gy and decreasing at higher doses. It should be noted that in most of the experimental works mentioned here, the dose of excitation was varied by changing the time of excitation, keeping the dose rate constant.

In previous work by Lawless et al. (2005), Pagonis et al. (2006), Chen et al. (2006), a non-monotonic dose dependence of TL and OSL has been explained by using a model consisting of two trapping states and two kinds of recombination center. In the non-monotonic dose dependence, increasing the dose of excitation increased the TL or OSL output up to a certain dose above which, the emitted signal declined with further dose. The effect as seen by the simulations occurred in the two ways the excitation dose was changed, namely, by changing the dose rate and keeping the time of excitation constant or by changing the time of excitation and keeping the dose rate constant. There are at least two differences between the previous and the present situations. In contrast to the two-trap two-center case discussed before, the model considered here includes two traps and only one center. As for the results, in the present case the dependence on the time of excitation with constant excitation dose rate gave a non-monotonic curve. On the other hand, with a constant time of excitation, the dose was changed by changing the dose rate and the dependence was found to be an increasing function which approaches saturation when the relevant trap was filled to capacity. Note that, in a sense, this is an expression of the possible dose-rate effect seen in some materials and also considered theoretically (see e.g. Chapter 8 in Chen and Pagonis, 2011).

Another work on the non-monotonic dose dependence of electron spin resonance (ESR) should be mentioned. It should be noted that the situation with ESR is similar to that of TL and OSL since the measured signal is proportional to the number of electrons trapped in the relevant trapping states. Based on a previous work by Euler and Kahan (1987), Woda and Wagner (2007) have offered a two-trap one center model to explain the non-monotonic dose dependence of ESR in Ge- and Ti-centers in quartz. The model assumes that in addition to the trapping of electrons from the conduction band into the active trap, the electrons may be depleted by recombination with free holes. As a result, the dose dependence of the concentration of electrons in the active trap is such that it increases at low doses, reaches a maximum at a certain dose and then declines gradually to zero following higher doses exposure. The differences between this model and the one presented here and between the results of the two models will be considered in the discussion below.

2. The model

Fig. 1 shows the model of two traps and one center. In this model, trap N_1 is considered to be closer to the conduction band and is assumed to be responsible for the TL or OSL signal during read-out. Trap N_2 is a deeper competitor that may be filling up during excitation in competition with N_1. n_1 (cm^{-3}) and n_2 (cm^{-3}) are the instantaneous occupancies of the traps concentrations N_1 (cm^{-3}) and N_2 (cm^{-3}) respectively. E (eV) and s (s^{-1}) are the activation energy and frequency factor of the N_1 trap; it is assumed that

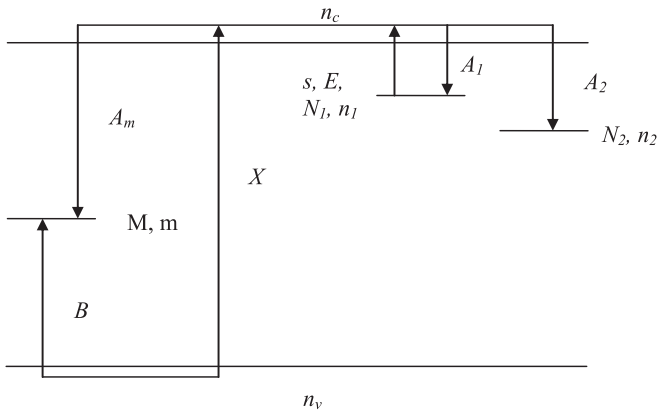

Fig. 1. Energy level diagram for the excitation of a two-trap one center system. The meanings of the shown parameters are given in the text.

N_2 is deep enough so that it does not release electrons thermally in ambient temperature. M (cm^{-3}) is the concentration of centers and m (cm^{-3}) its instantaneous occupancy. n_c (cm^{-3}) and n_v (cm^{-3}) are the instantaneous concentrations of free electrons and holes in the conduction and valence bands, respectively. A_1 ($cm^3\ s^{-1}$) and A_2 ($cm^3\ s^{-1}$) are the retrapping probability coefficients into N_1 and N_2, respectively. B ($cm^3\ s^{-1}$) is the probability coefficient for trapping free holes in the centers and A_m ($cm^3\ s^{-1}$) is the recombination probability of free electrons with trapped holes in centers. X ($cm^{-3}\ s^{-1}$) is the rate of production of electron–hole pairs by the ionizing radiation, proportional to the dose rate of the excitation. D (cm^{-3}) is the total number of electron–hole pairs per cm^3 produced by the irradiation, proportional to the total dose applied, given by $D = X \cdot t_D$ where t_D (s) is the time of excitation.

The set of coupled differential equations governing the process during excitation is

$$\frac{dn_1}{dt} = A_1(N_1 - n_1)n_c - sn_1 \exp(-E/kT), \tag{1}$$

$$\frac{dn_2}{dt} = A_2(N_2 - n_2)n_c, \tag{2}$$

$$\frac{dm}{dt} = B(M - m)n_v - A_m m n_c, \tag{3}$$

$$\frac{dn_v}{dt} = X - B(M - m)n_v, \tag{4}$$

$$\frac{dn_c}{dt} = \frac{dm}{dt} + \frac{dn_v}{dt} - \frac{dn_1}{dt} - \frac{dn_2}{dt}. \tag{5}$$

T (K) is the absolute temperature, t (s) is the time and k ($eV\ K^{-1}$) is Boltzmann's constant.

3. Numerical results

The set of Eqs. (1)–(5) has been solved numerically for chosen sets of parameters, using the Matlab ode15s solver, designed to solve "stiff" sets of simultaneous ordinary differential equations. The trapping parameters used for the simulation of Fig. 2 are $N_1 = 10^{13}\ cm^{-3}$, $N_2 = 10^{14}\ cm^{-3}$, $M = 10^{15}\ cm^{-3}$, $A_m = 10^{-14}\ cm^3\ s^{-1}$; $A_1 = 10^{-16}\ cm^3\ s^{-1}$; $A_2 = 10^{-15} cm^3\ s^{-1}$; $B = 10^{-13}\ cm^3\ s^{-1}$; $E = 1.4$ eV; $s = 10^{12}\ s^{-1}$; $T = 300$ K; $X = 10^3\ cm^{-3}\ s^{-1}$. The activation energy chosen here is rather big so that the rate of release of trapped electrons is very small. Also, the excitation rate X is rather small, $10^3\ cm^{-3}\ s^{-1}$. With these parameters, the accumulation of electrons in the active trap n_1 is seen to be linear with the excitation time up to ~2×10^9 s ~60 years. Note that the final occupancy of this trap is under $2 \times 10^{10}\ cm^{-3}$, less than 0.2% of the capacity of the trap.

The simulation was continued to significantly longer times of excitation, up to more than 10^{13} s ~3×10^5 years, as shown in Fig. 3. In order to cover this long range of excitation time, the time axis is shown on a logarithmic scale. Due to the thermal loss of electrons at long time and the slow rate of electron–hole production, the net filling of electrons in N_1 deviates from linearity, reaches a maximum at ~5×10^{11} s and then declines. At longer excitation time of ~2×10^{12} s, an equilibrium between excitation and thermal leakage is reached. Note that in this case, the equilibrium level is significantly lower than the saturation value of the trap at ~3.2% of the full capacity. The relation between this equilibrium value and the relevant trapping parameters is given below. Note that with these parameters, at the equilibrium range, n_2 has reached its saturation value of $1 \times 10^{14}\ cm^{-3}$ and m is $1.0032 \times 10^{14}\ cm^{-3}$ which is equal to $n_1 + n_2$. Note also that evaluated n_c and n_v are negligibly small as compared to the trapping concentrations.

Another example is shown in Fig. 4. The trapping parameters are the same as before except that the activation energy is significantly smaller, $E = 0.9$ eV and the rate of production of electron–hole pairs is significantly higher, $X = 10^9\ cm^{-3}\ s^{-1}$. The peak in the curve here appears at a much shorter period of time, under 10^4 s and the equilibrium value sets in after ~10^6 s. The equilibrium value here is only $1.3178 \times 10^9\ cm^{-3}$, ~0.013% of the capacity of the trap. Here too, at the equilibrium range n_2 is at full capacity of $10^{14}\ cm^{-3}$ and m has also the same value of $10^{14}\ cm^{-3}$.

In Fig. 5, the rates of filling of trap n_1 and its thermal emptying as seen in Eq. (7) below are shown as a function of time. The trapping parameters are the same as in Fig. 3 except that the "dose rate" is two orders of magnitude smaller, X = 10 $cm^{-3}\ s^{-1}$. As could be expected, the two curves intersect at the point of the maximum of $sn_1 \exp(-E/kT)$ which, of course, is the point of maximum of n_1 since the temperature is kept constant. Also, the two curves

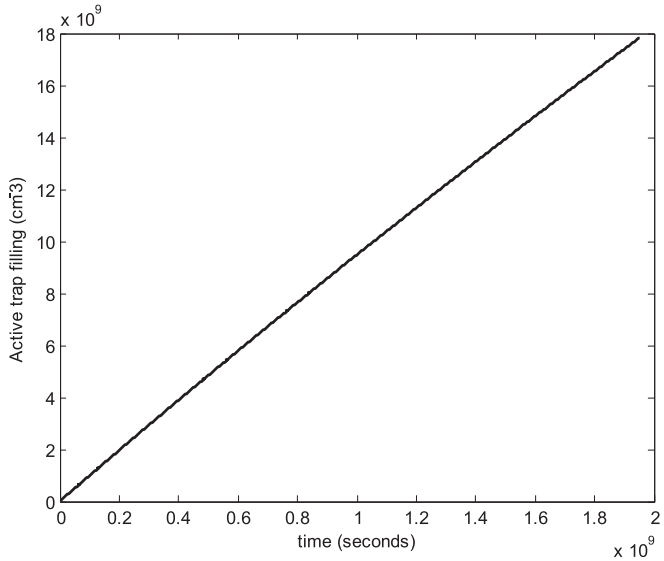

Fig. 2. For the set of parameters given in the text, the simulated dose dependence of the filling of active trap is shown in the short-time range, up to ~2×10^9 s.

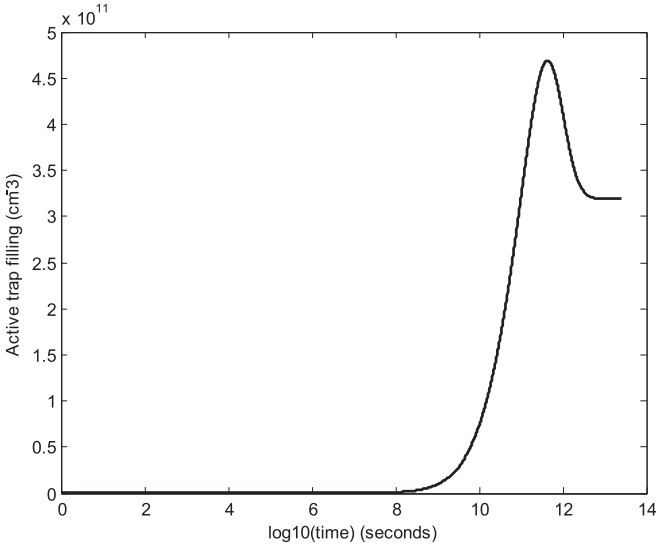

Fig. 3. With the same set of parameters as in Fig. 2, the simulated time dependence is shown up to ~5×10^{13} s. Note the logarithmic time scale.

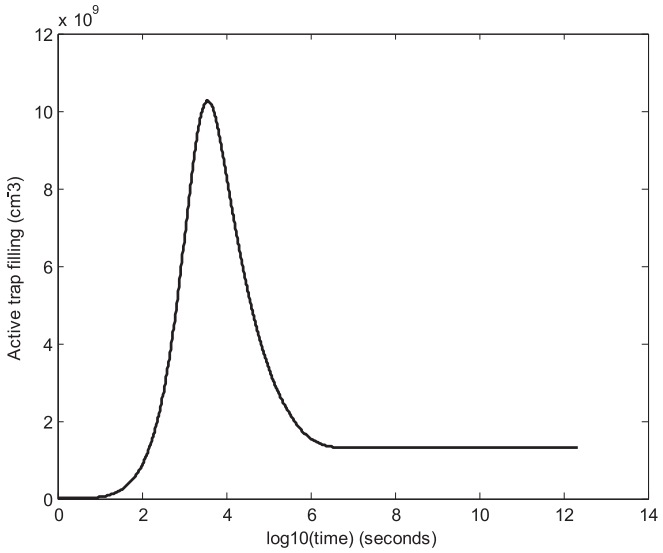

Fig. 4. Simulations of the time dependence with the same set of parameters, except that $E = 0.9$ eV and the rate of production of electron–hole pairs is 10^9 cm^{-3} s^{-1}.

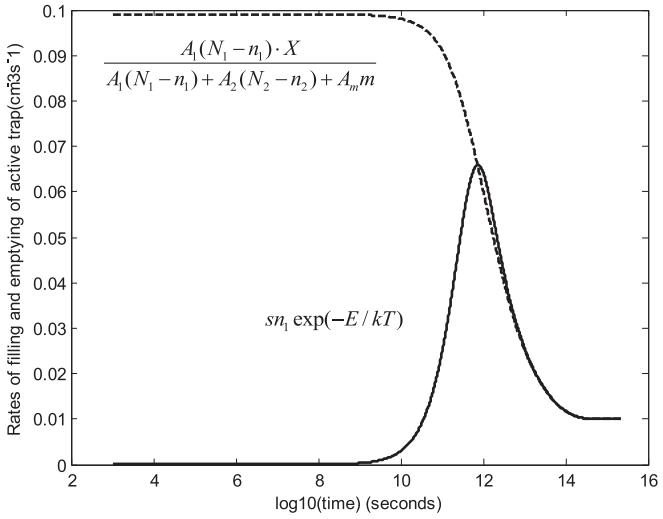

Fig. 5. With the same parameters as in Fig. 3, but with significantly smaller rate of excitation, $X = 10$ cm^{-3} s^{-1}, the dependence on time of the filling of n_1, $\frac{A_1(N_1-n_1)\cdot X}{A_1(N_1-n_1)+A_2(N_2-n_2)+A_m m}$ is shown by the dashed line and the thermal emptying, $sn_1 \exp(-E/kT)$ is depicted by the solid line.

coincide at the long-time end where, as a result, n_1 levels off.

It should be mentioned that the effect described here is rather similar to the effect of non-monotonic dose dependence described in the literature. Changing the time of excitation with a constant dose rate indeed changes the total dose applied to the sample. In the previous simulations (Lawless et al., 2005; Chen et al., 2006; Pagonis et al., 2006), however, with a two-trap two-center model, the non-monotonic dependence was observed both when the time of excitation was varied and when the dose-rate was changed with a constant time of excitation. Fig. 6 depicts the results of simulations of the latter case. With the same parameters as in Fig. 3, the time of excitation was kept unchanged at 10 s and the dose rate X was varied in a broad range so that the total "dose" changed by many orders of magnitude. As seen in the results, the filling of the active trap changed from nearly zero at $D \approx 10^{12}$ cm^{-3} to full saturation value of $n_1 \approx N_1$ at $D \approx 10^{17}$ cm^{-3}. The non-monotonic

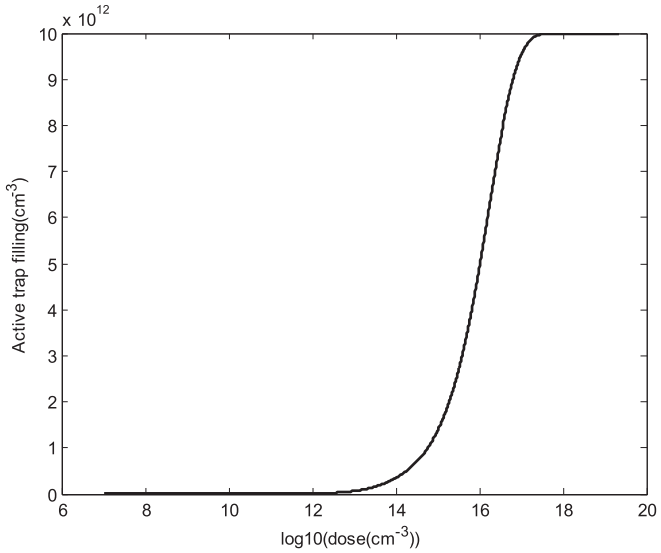

Fig. 6. With the same set of parameters as in Fig. 3, the simulations have been conducted with a constant time of $t_D = 10$ s and varying dose rate X. The dose is given on a logarithmic scale. Note that D (cm^{-3}) is actually the total number of electron–hole pairs per cm^3 produced by the irradiation, proportional to the total dose applied, as explained in the text.

effect seen with the change of time of excitation is not seen at all when the dose varies by changing the dose rate of excitation, indicating that the effect observed here has to do with the competition between excitation and thermal bleaching. This point will be elaborated upon below.

Finally, Fig. 7 shows a comparison between the results of n_1 from the numerical solution of Eqs. (1)–(5) and the analytical approximation given by Eq. (A25) in the Appendix below. The parameters are the same as in Fig. 4, except that in order to have the occupancies in the two traps be far from saturation as required by the

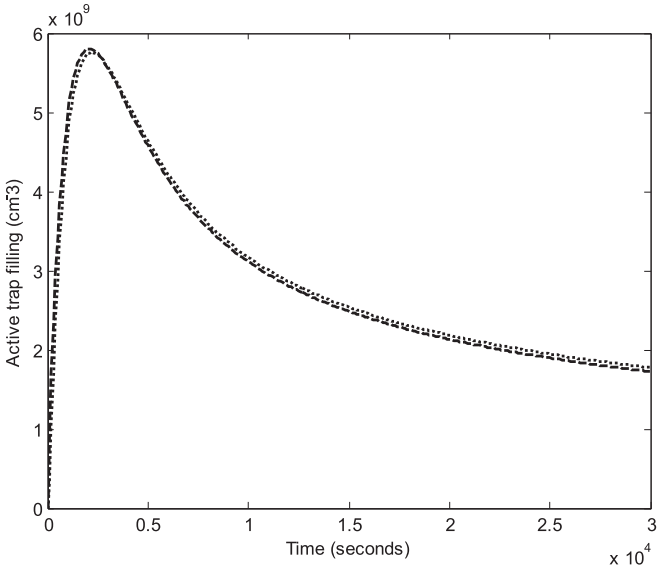

Fig. 7. Comparison between the results of n_1 as a function of time to those reached by the approximation given by Eq. (A25). The parameters are the same as in Fig. 4 with A_1 and A_2 reduced by a factor of 10, namely, $A_1 = 10^{-17}$ cm^3 s^{-1}; $A_2 = 10^{-16}$cm^3 s^{-1}, so that we avoid saturation of the traps, namely, $n_1 << N_1$ and $n_2 << N_2$. The dotted line depicts the results of solving the differential equations and the dashed line shows the results by Eq. (A25).

approximation elaborated upon in the Appendix, the two retrapping/trapping probabilities A_1 and A_2 are reduced by a factor of 10. The dashed line gives the approximate analytical solution and the dotted line the numerical solution of the equations. The agreement between the two is seen to be very good. Note that the time scale here is linear.

4. Discussion

In this work, we have considered the dependence of the filling of a trap at different times of excitation in a model with two traps and one center. For chosen plausible sets of trapping parameters, the relevant sets of simultaneous equations have been solved numerically. As shown in Figs. 3 and 4, the concentration n_1 reached a maximum and then declined and after a longer period of time reached a constant equilibrium value. Let us consider this equilibrium value in the two given examples. The rate of release of electrons from the trap is given by $s \cdot n \cdot \exp(-E/kT)$. The rate of production of electrons in the conduction band is X. These electrons are distributed between falling into N_1, N_2 and recombination with trapped holes in the centers. Therefore, the ratio of electrons trapped in N_1 is

$$R = \frac{A_1(N_1 - n_1)}{A_1(N_1 - n_1) + A_2(N_2 - n_2) + A_m m}. \quad (6)$$

Therefore, the equilibrium condition here is

$$s \cdot n_1 \cdot \exp(-E/kT) = X \cdot R. \quad (7)$$

Let us consider the consistency between the calculated values of the chosen parameters and the calculated occupancies of traps and centers. The evaluated occupancies are $n_1 = 3.1944 \times 10^{11}$ cm^{-3}, $n_2 = 10^{14}$ cm^{-3} and $m = 1.0032 \times 10^{14}$ cm^{-3} n_c and n_v are negligibly small. Since $n_2 \approx N_2$, the second term in the denominator is negligibly small. Also, since $N_1 >> n_1$, $A_1(N_1\text{-}n_1) \approx A_1 N_1 = 10^{-16} \times 10^{13} = 10^{-3}$ s^{-1}. Also, $A_m m \approx 10^{-14} \times 10^{14}$ s^{-1} $= 1$ s^{-1} $>> A_1 N_1$. With these parameters and results, the equilibrium condition can be written as

$$n_1 \approx (X/s) \cdot (A_1 N_1 / A_m m) \cdot \exp(E/kT). \quad (8)$$

Inserting the given values on the right-hand side yields $n_1 \approx 3.31 \times 10^{11}$ cm^{-3}, within ~3.5% of the numerically calculated value. Note that here, equilibrium is reached after ~3×10^{12} s ~10^5 years.

With the parameters yielding Fig. 4, in particular with the low value of $E = 0.9$ eV, equilibrium is reached after a much shorter time, ~3×10^6 s ~35 days. The value of n_1 from the numerical solution of the equations is 1.3178×10^{10} cm^{-3}. The other two occupancies are $n_2 = m = 10^{14}$ cm^{-3}. Inserting the relevant parameters in Eq. (8) yields here $n_1 = 1.318 \times 10^{10}$ cm^{-3}, in excellent agreement with the numerically computed value.

The differences between the present situation and the previously reported model of non-monotonic dose dependence of TL and OSL (Chen et al., 2006) are two. The model here is more concise, including two trapping states and only one recombination center. As for the results, in the previous model, the non-monotonic dependence was found in both ways of changing the dose, namely, by changing the dose rate or by varying the time of excitation. Here, a non-monotonic dependence is seen as a function of the time of excitation with a constant dose rate, and it does not take place with a constant time of excitation and increasing dose rate (see Eq. (A30) below and the accompanying discussion). This result seems plausible since the decline toward an equilibrium value is associated here with the thermal fading due to the slow release of electrons from traps during a long, slow excitation. One may expect a similar effect in cases where the fading of the signal is anomalous, i.e. non thermal, but this has not been pursued in the present work. As for a comparison between the present model and that by Woda and Wagner (2007) mentioned in the Introduction, in addition to the fact that these authors concentrate on consequences in ESR one should note the following. In addition to the filling of active traps by the dose, Woda and Wagner assume depletion of the traps by recombination with free holes whereas here, we assume that electrons are depleted by thermal eviction into the conduction band. These authors also assume a loss of free electrons and holes by direct band-to-band recombination, a transition which is usually considered to have a very low probability (see e.g. Pilkuhn, 1976). Consequently, their numerical results show a decline down to zero in the active trap occupancy whereas in our case the decline is toward a constant equilibrium value. Also, in our work, the emphasis is on the dependence on the time of excitation whereas Woda and Wagner consider the dose response.

It should be mentioned that in the present work, we did not deal directly with the TL or OSL signal but rather, with the filling of the n_1 trap. However, at least in the cases shown, at the end of radiation, the other trap, n_2 was full to capacity with electrons, so that no retrapping into N_2 is expected during readout and a subsequent TL or OSL measurement would yield results proportional to n_1. Also, as mentioned in the Introduction, these results may possibly be relevant to the dose dependence of ESR.

Appendix A. Quasi-analytical derivation

In order to get a quasi-analytical solution of Eqs. (1)–(5), we make the following simplifying assumptions:

1. Free electrons and free holes are quasi steady.
2. The populations of both traps are well below capacity.
3. Trap N_1 is small compared to N_2. In fact, we assume $N_1 << N_2$ and also $A_1 N_1 << A_2 N_2$.

Let us consider first the solution of Eqs. (1)–(5) for the major species m and n_2, assuming that n_1 is small. More specifically, we assume that A_1 and N_1 are small enough so that the net flux into N_1 is always smaller than that into N_2

$$|A_1(N_1 - n_1)n_c - \alpha n_1| << A_2(N_2 - n_2)n_c, \quad (A1)$$

where $\alpha = s \cdot \exp(-E/kT)$. In this case Eqs. (1)–(5) simplify to the one-trap one-center situation, namely

$$\frac{dn_2}{dt} = A_2(N_2 - n_2)n_c, \quad (A2)$$

$$\frac{dm}{dt} = B(M - m)n_v - A_m m n_c, \quad (A3)$$

$$\frac{dn_v}{dt} = X - B(M - m)n_v, \quad (A4)$$

$$\frac{dn_c}{dt} = X - A_2(N_2 - n_2)n_c - A_m m n_c. \quad (A5)$$

To simplify this further, let us assume that free electrons and free holes are quasi-steady (see (A6) and (A7)) and that the population of trap 2 is well-below saturation. Thus, for free electrons we assume

$$\left|\frac{dn_c}{dt}\right| << A_2(N_2 - n_2)n_c. \tag{A6}$$

With the parameters chosen for the simulations, $1/(A_2N_2) = 10$ s, and the quasi-steady assumption for free electrons will be valid for excitation periods much longer than 10 s.

For free holes, let us assume

$$\left|\frac{dn_v}{dt}\right| << B(M - m)n_v. \tag{A7}$$

Since with the parameters chosen, $1/(BM) = 0.01$ s, this will be valid for excitation periods much longer than 10 ms, which applies to all the results in the paper.

For the population of the second trap, assume that the total dose is low enough so that $n_2 << N_2$. With these assumptions, Eqs. (A2–A5) simplify to

$$\frac{dn_2}{dt} = A_2N_2n_c, \tag{A8}$$

$$\frac{dm}{dt} = B(M - m)n_v - A_mmn_c, \tag{A9}$$

$$n_v = \frac{X}{B(M - m)}, \tag{A10}$$

$$n_c = \frac{X}{A_2N_2 + A_mm}. \tag{A11}$$

The differential equations can be immediately integrated to yield:

$$m = n_2 = \frac{A_2}{A_m}N_2\left(\sqrt{1 + t/\tau} - 1\right), \tag{A12}$$

where the abbreviation τ is defined as

$$\tau = \frac{A_2N_2}{2A_mX}. \tag{A13}$$

For short times, $t << \tau$, Eq. (A12) shows that m and n_2 rise sublinearly with time. The physical meaning is that for $t << \tau$, the hole population of the center, m, is still too small for the center to compete with N_2 for the capture of free electrons, $A_mm << A_2N_2$. For $t >> \tau$, the hole population of the center is large enough so that the center attracts free electrons at a greater rate than the second trap.

Let us consider now the approximate solution for the occupancy of the smaller trap n_1. Substituting from Eq. (A11) into Eq. (1), we have

$$\frac{dn_1}{dt} = \frac{A_1(N_1 - n_1)}{A_2N_2 + A_mm}X - \alpha n_1. \tag{A14}$$

To further simplify this, let us assume that the population of the first peak is well below capacity, namely, $n_1 << N_1$. Thus,

$$\frac{dn_1}{dt} = \frac{A_1N_1}{A_2N_2 + A_mm}X - \alpha n_1. \tag{A15}$$

Substituting the value for m from Eq. (A12) into (A15), we have

$$\alpha n_1 + \frac{dn_1}{dt} = \frac{A_1N_1}{A_2N_2}\frac{X}{\sqrt{1 + t/\tau}}. \tag{A16}$$

Let us multiply both sides of Eq. (A15) by $\exp(\alpha t)$,

$$\alpha n_1e^{\alpha t} + \frac{dn_1}{dt}e^{\alpha t} = \frac{A_1N_1}{A_2N_2}\frac{Xe^{\alpha t}}{\sqrt{1 + t/\tau}}. \tag{A17}$$

This equation can be rewritten as

$$\frac{d}{dt}\left(n_1e^{\alpha t}\right) = \frac{A_1N_1}{A_2N_2}\frac{Xe^{\alpha t}}{\sqrt{1 + t/\tau}}. \tag{A18}$$

Integrating both sides with respect to time yields

$$n_1e^{\alpha t} = \frac{A_1N_1}{A_2N_2}\int_0^t \frac{Xe^{\alpha t'}}{\sqrt{1 + t'/\tau}}dt'. \tag{A19}$$

Let us define a new variable,

$$u \equiv \sqrt{\alpha\tau}\sqrt{1 + t/\tau}. \tag{A20}$$

Rearranging Eq. (A20), we find

$$t = \frac{u^2}{\alpha} - \tau. \tag{A21}$$

Differentiating Eq. (A21) gives

$$dt = \frac{2udu}{\alpha}. \tag{A22}$$

Substituting Eqs. (A21) and (A22) into (A19) yields

$$n_1 = 2\frac{A_1N_1}{A_2N_2}X\sqrt{\frac{\tau}{\alpha}}e^{-\alpha(t+\tau)}\int_{\sqrt{\alpha\tau}}^{\sqrt{\alpha(t+\tau)}} e^{u^2}du. \tag{A23}$$

Rearranging, one gets

$$n_1 = 2\frac{A_1N_1}{A_2N_2}\sqrt{\frac{\tau}{\alpha}}X\left[e^{-\alpha(t+\tau)}\int_0^{\sqrt{\alpha(t+\tau)}} e^{u^2}du - e^{-\alpha(t+\tau)}\int_0^{\sqrt{\alpha\tau}} e^{u^2}du\right], \tag{A24}$$

which, in turn can be written as

$$n_1 = 2\frac{A_1N_1}{A_2N_2}X\sqrt{\frac{\tau}{\alpha}}\left[F\left(\sqrt{\alpha(t+\tau)}\right) - e^{\alpha t}F\left(\sqrt{\alpha\tau}\right)\right], \tag{A25}$$

where F is the Dawson Integral (see, e.g., Abramowitz and Stegun, 1970),

$$F(x) = e^{-x^2}\int_0^x e^{x'^2}dx'. \tag{A26}$$

With regard to the equilibrium value of n_1 reached at long times, as expressed in Eq. (8) and the above mentioned numerical results of this equilibrium value, the asymptotic behavior of the Dawson Integral is

$$F(x) \approx \frac{1}{2x} \quad for \quad x >> 1. \tag{A27}$$

Thus, for large values of $\alpha\tau$, Eq. (A25) can be approximated by

$$n_1 \approx \frac{1}{\alpha}\frac{A_1N_1}{A_2N_2}\frac{X}{\sqrt{1 + t/\tau}} \quad for \quad \alpha t >> 1. \tag{A28}$$

Using Eq. (A12), we can rewrite this as

$$n_1 \approx \frac{A_1 N_1 X}{\alpha(A_2 N_2 + A_m m)} \quad for \quad \alpha t >> 1, \tag{A29}$$

which is actually the same as Eq. (8). Note that this is the value that one would obtain from Eq. (A15) by assuming that n_1 is quasi-steady.

By substituting from Eq. (A13) into Eq. (A28) we get

$$n_1 \approx \frac{1}{\alpha}\frac{A_1 N_1}{A_2 N_2}\frac{X}{\sqrt{1+\frac{2A_m}{A_2 N_2}Xt}}. \quad for \quad \alpha t >> 1 \tag{A30}$$

Thus, for $\alpha t >> 1$, for fixed dose rate X, increasing t causes n_1 to decrease, which is associated with the non-monotonic effect, in agreement with Figs. (3–5). For a fixed t, increasing X causes n_1 to increase, in agreement with the numerical results in Fig. 6.

References

Abramowitz, M., Stegun, I.A., 1970. Handbook of Mathematical Functions. U.S. Government Printing Office, Washington DC.

Cameron, J.R., Suntharalingam, N., Kenney, G.N., 1966. Thermoluminescent Dosimetry. The University of Wisconsin Press.

Charlesby, A., Partridge, R.H., 1963. The thermoluminescence of irradiated polyethylene and other polymers. Proc. Roy. Soc. Lond. Ser. A 271, 170–206.

Chen, R., Lo, D., Lawless, J.L., 2006. Non-monotonic dose dependence of thermoluminescence. Radiat. Prot. Dosim. 119, 33–36.

Chen, R., Pagonis, V., 2011. Thermally and Optically Stimulated Luminescence: a Simulation Approach. Wiley and Sons, Chichester.

Damm, J.Z., Opyrchal, H., 1975. On the origin of thermoluminescence in γ-irradiated pure and metal doped potassium chloride crystals. Part I. Cryst. Latt. Def. 6, 21–26.

David, M., Sunta, C.M., Ganguly, A.K., 1977. Thermoluminescence of quartz: Part II-Sensitisation by thermal treatment. Ind. J. Pure Appl. Phys. 15, 277–288.

David, M., Sunta, C.M., 1981. Thermoluminescence of quartz-Part VI: effect of ultraviolet rays. Ind. J. Pure Appl. Phys. 19, 1041–1047.

Euler, F.K., Kahan, A., 1987-II. Radiation effects and anelastic loss in germanium-doped quartz. Phys. Rev. 35, 4351–4359.

Gulamova, R.R., Gasanov, E.M., Sazonova, E.V., 1993. Radiation-induced defect formation in silica glasses. Phys. Stat. Sol.(a) 135, 109–117.

Halperin, A., Chen, R., 1966. Thermoluminescence in semiconducting diamonds. Phys. Rev. 148, 839–845.

Horowitz, Y.S., Moscovitch, M., Wilt, M., 1986. Computerized glow curve deconvolution applied to ultralow dose LiF thermoluminescence dosimetry. Nucl. Inst. Methods Phys. Res. Sect. A Accel. Spectrom. Detect. Assoc. Equip. 244, 556–564.

Ichikawa, Y., 1969. Thermoluminescence of natural quartz irradiated by gamma rays. Jpn. J. Appl. Phys. 7, 220–226.

Jain, V.K., Kathuria, S.P., Ganguly, A.K., 1975. Radiation damage in thermoluminescenct LiF TLD-phosphor. J. Phys. C. Solid State Phys. 8, 2191–2197.

Lawless, J.L., Chen, R., Lo, D., Pagonis, V., 2005. A model for non-monotonic dose dependence of thermoluminescence (TL). J. Phys. Condens. Matter 17, 737–753.

Pagonis, V., Chen, R., Lawless, J.L., 2006. Nonmonotonic dose dependence of OSL intensity due to competition during irradiation and readout. Radiat. Meas. 41, 903–909.

Pilkuhn, M.H., 1976. Electron-hole recombination. In: Proc. 13th Int. Conf. Phys. of Semiconductors, pp. 61–70.

Schulman, J.H., Etzel, H.W., Allard, J.G., 1957. Application of luminescence changes in organic solids to dosimetry. J. Appl. Phys. 28, 792–795.

Vij, A., Lochab, S.P., Kumar, R., Singh, N., 2009. Thermoluminescence study of UV irradiated Ce doped SrS nanostructures. J. Alloys Compd. 486, 554–558.

Woda, C., Wagner, G.A., 2007. Non-monotonic dose dependence of the Ge- and Ti-centers in quardz. Radiat. Meas. 42, 1441–1452.

Yukihara, E.G., Whitley, V.H., Polf, J.C., Klein, D.M., McKeever, S.W.S., Akselrod, A.E., Akselrod, M.S., 2003. The effects of deep trap population on the thermoluminescence of Al2O3:C. Radiat. Meas. 37, 627–638.